Since January 2020 Elsevier has created a COVID-19 resource centre with free information in English and Mandarin on the novel coronavirus COVID-19. The COVID-19 resource centre is hosted on Elsevier Connect, the company's public news and information website.

Biomedicine & Pharmacotherapy 149 (2022) 112872

Contents lists available at ScienceDirect

Biomedicine & Pharmacotherapy

journal homepage: www.elsevier.com/locate/biopha

Lithium salts as a treatment for COVID-19: Pre-clinical outcomes

O. Soriano-Torres [a,*], E. Noa Romero [b], NL González Sosa [b], JM Enríquez Puertas [b], A. Fragas Quintero [b], M. García Montero [b], D. Martín Alfonso [b], Y. Infante Hernández [b], M. Lastre [a], L. Rodríguez-Pérez [a], Y. Borrego [a], VE González [a], IG Vega [a], R. Ramos Pupo [a,c], LM Reyes [a], MT Zumeta Dubé [d], Amaro Hernández I [d], I. García de la Rosa [e], A. Minguez Suárez [f], LA Alarcón Camejo [f], M. Rodríguez [b], R. Oliva Hernández [g], CE Rudd [h,i,j], O. Pérez [a,*]

[a] Immunology Department, Instituto de Ciencias Básicas y Preclínicas "Victoria de Girón", Universidad de Ciencias Médicas de La Habana, Havana, Cuba
[b] Civilian Defense Scientific Research Center, Mayabeque, Cuba
[c] Biomedical Research Institute (BIOMED), Faculty of Medicine and Life Science, Hasselt University, Belgium
[d] Histology Department, Instituto de Ciencias Básicas y Preclínicas "Victoria de Girón", Universidad de Ciencias Médicas de La Habana, Havana, Cuba
[e] Immunoassay Center, Havana, Cuba
[f] MedSol Laboratories, Havana, Cuba
[g] Finlay Vaccine Institute, Havana, Cuba
[h] Centre de Recherche Maisonneuve-Rosemont Hospital (CR-HMR), Montreal, QC H1T 2M4, Canada
[i] Département de Medicine, Université de Montréal, Montreal, QC H3C 3J7, Canada
[j] Department of Medicine, Division of Endocrinology & Medical Biochemistry, McGill University Health Center, Canada

ARTICLE INFO

Keywords:
SARS-CoV-2
COVID-19
Lithium
Pre-clinical trial
Inflammation

ABSTRACT

Introduction: Identifying effective drugs for Coronavirus disease 2019 (COVID-19) is urgently needed. An efficient approach is to evaluate whether existing approved drugs have anti-SARS-CoV-2 effects. The antiviral properties of lithium salts have been studied for many years. Their anti-inflammatory and immune-potentiating effects result from the inhibition of glycogen synthase kinase-3.

Aims: To obtain pre-clinical evidence on the safety and therapeutic effects of lithium salts in the treatment of COVID-19.

Results: Six different concentrations of lithium, ranging 2–12 mmol/L, were evaluated. Lithium inhibited the replication of SARS-CoV-2 virus in a dose-dependent manner with an IC_{50} value of 4 mmol/L. Lithium-treated wells showed a significantly higher percentage of monolayer conservation than viral control, particularly at concentrations higher than 6 mmol/L, verified through microscopic observation, the neutral red assay, and the determination of N protein in the supernatants of treated wells. Hamsters treated with lithium showed less intense disease with fewer signs. No lithium-related mortality or overt signs of toxicity were observed during the experiment. A trend of decreasing viral load in nasopharyngeal swabs and lungs was observed in treated hamsters compared to controls.

Conclusions: These results provide pre-clinical evidence of the antiviral and immunotherapeutic effects of lithium against SARS-CoV-2, which supports an advance to clinical trials on COVID-19's patients.

1. Introduction

SARS-CoV-2 causes a severe respiratory disease (COVID-19) characterized by significant deregulation of the immune system with overproduction of pro-inflammatory cytokines (cytokine storm) [1]. It shares about 80% genetic homology with SARS-CoV causing the severe acute respiratory syndrome epidemic in 2003 [2] that began in the Chinese province of Guangdong [3]. Like other coronaviruses, its viral particles include genetic material of a single chain of positive sense ribonucleic acid (RNA) and structural proteins necessary for the invasion of host cells, which include the surface or spike glycoprotein (S), the membrane glycoprotein (M), the envelope glycoprotein (E), the nucleocapsid glycoprotein (N) and the dimeric glycohemagglutinin-esterase [4]. Once inside the cells, the infective RNA encodes structural and

* Corresponding authors.
E-mail addresses: ormany87@gmail.com (O. Soriano-Torres), oliver.perez@infomed.sld.cu (O. Pérez).

https://doi.org/10.1016/j.biopha.2022.112872
Received 10 January 2022; Received in revised form 20 March 2022; Accepted 23 March 2022
Available online 25 March 2022

non-structural proteins that control assembly, transcription and viral replication [5]. The N protein supports the viral RNA and is involved in its packaging [6,7]. The native hypo-phosphorylated form of this protein favors its binding to genetic material [8], forming RNA-protein condensates.

Coronaviruses require a host's kinase termed glycogen synthase kinase-3 (GSK-3) activity for its replication. This enzyme phosphorylates the N glycoprotein [9,10] reducing RNA-protein interactions, forming a looser conglomerate [6], which favors the genome transcription, an essential step in the generation of long sub-genomic and genomic mRNAs that code for structural proteins in the cell cytosol during viral replication [9]. GSK-3 is constitutively expressed in all mammalian cells [11] and is important in several biological processes [12]. At the immune level, inhibition of cytosolic and nuclear GSK-3 increases the transcription of TBX21 (also called T-box expressed in T cells, Tbet), which in turn suppresses the transcription and expression of programmed cell death protein 1 (PD-1) in activated lymphocytes, in particular, TCD8 + lymphocytes [13]. PD-1 is a cell surface receptor expressed transiently in multiple cells of the immune system, including T and B lymphocytes [14], macrophages [15], natural killer (NK) cells [16], and dendritic cells [17]. It functions as an immune checkpoint and plays an important role in the negative regulation of the immune system [18]. Blockade of PD-1 is known to increase self-renewal and proliferation of stem-like TCD8 in lymph nodes, increasing effector functions of cytolytic T lymphocytes (CTL) against infections and cancer [19,20]. The same inhibitory effect on the expression of another inhibitory receptor LAG3 has been seen [21]. GSK-3 inhibition down-regulates the inhibitory co-receptor LAG-3 on CD4 + and CD8 + T-cells to enhance anti-viral and anti-tumor immunity [21,22].

Lithium was the first natural GSK-3 inhibitor described [23]. In psychiatry, lithium has been used as a specific treatment for mania since 1949 [24]. The antiviral properties of lithium have been studied since 1980 [25]. Although a detailed review of lithium antiviral effects lies outside the scope of this work, some other potential mechanisms might be relevant besides the GSK-3 inhibition, as the regulation of autophagy, the inhibition of the phosphatidylinositol signaling pathway [26] and inhibition of RNA polymerases [27]. *In vitro* experiments have demonstrated that, at non-toxic concentrations in cell cultures, it is capable of inhibiting the replication of different viral types, including herpes viruses [25], coxsackievirus [28,29], hepatitis C virus [30] and coronaviruses [31–33].

Clinical administration of lithium is typically in the form of salts (lithium carbonate) as oral tablets (in doses of 0.4–2.0 g/day) and its effective therapeutic range lies between 0.5 and 1.2 mmol/L in blood serum [34]. Besides its antiviral properties, lithium has immunomodulatory/anti-inflammatory effects [35–39]. Despite the longstanding use of lithium salts in humans, including a proof of concept in COVID-19 [40], no pre-clinical trials have been conducted.

The study of the characteristics of viruses and the evaluation of drugs with antiviral properties is carried out first in cell cultures. Vero E6 cells are African green monkey (*Cercopithecus aethiops*) kidney epithelial cells commonly used in virology studies. Research projects on SARS-CoV and SARS-CoV-2 have been carried out using these cells because of their high expression of angiotensin-converting enzyme 2 (ACE2) receptor and their ability to support a high rate of viral replication [41–44].

The availability and use of animal models in the study of the pathogenesis of COVID-19 is also of great significance in the pre-clinical evaluation of new therapeutics. Syrian hamsters (*Mesocricetus auratus*) are widely used as experimental animals and, due to the high degree of homology of its ACE2 receptor with that of humans, they have been used previously in SARS studies [45,46], and have been defined as a bio-model for SARS-CoV-2 studies [47–50]. After intranasal inoculation of hamsters with SARS-CoV-2, moderate interstitial pneumonia occurs with high viral load in lungs, although only a mild and rapidly resolving disease is observed [47].

Even though most studies in hamsters have been carried out using high infectious doses (10^3–10^5 mean tissue culture infectious dose, $TCID_{50}$) [48,50,51], it has been defined that the mean infective dose (ID_{50}) is only 5 $TCID_{50}$ [47]. The most common manifestations of the disease in hamsters are weight loss, ruffle fur, lethargy (reduced mobility), hunched back and polypnea [47,49–51].

The present work aims to obtain pre-clinical evidence on the safety and therapeutic effects of lithium salts in the treatment of COVID-19.

2. Materials and methods

2.1. Reagents

Minimal Essential Medium (MEM) (Gibco, Paisley, UK), gentamicin and L-glutamine (Capricorn Scientific, Ebsdorfergrund, Germany), lithium chloride monohydrate ($LiCl*H_2O$), sulfuric acid, sodium bicarbonate, balanced salts solution (BSS) and Tween-20 (Merck, Darmstadt, Germany), bovine serum albumin (BSA), fetal bovine serum (FBS) and horseradish peroxidase (Sigma-Aldrich, St. Louis, MO, USA), neutral red (NR) (PanReac AppliChem, Darmstadt, Germany), tetramethylbenzidine (TMB) (Sigma-Aldrich, Darmstadt, Germany), anti-SARS-CoV-2N protein monoclonal antibody (CBSS NCoV) (Center for Genetic Engineering and Biotechnology, Sancti-Spíritus, Cuba) and lithium carbonate tablets (250 mg) (MedSol Laboratories, Havana, Cuba) were used.

2.2. Cell culture, virus strain, and animal model

Vero E6 cells (ATCC CRL-1586, CICDC) cryo-preserved at − 80 °C were defrosted and then subcultured twice a week at 3×10^4 cell/cm^2 in MEM supplemented with 10% FBS, 2 mmol/L of 1% L-glutamine and 7.5% sodium bicarbonate. Cells were seeded in 96-well flat-bottom plates (Nunclon Delta Surface, Roskilde, Denmark) at a density of 20×10^3 cells/well in 100 μL of supplemented MEM and grown overnight at 37 °C in 5% CO_2 atmosphere, with 4% FBS. SARS-CoV-2 strain (CUT-2010–2025) isolated at CICDC from a Cuban patient nasopharyngeal swab and stored at − 80°C was used. The $TCID_{50}$ was determined by end point microtitration in Vero E6 cells at 10×10^3 cells/well [52,53].

Twenty-four female Syrian hamsters from the National Center for the Production of Laboratory Animals (CENPALAB, Havana, Cuba), with 4–6 weeks old reception age, 70–80 g at the beginning of the experiments were used. Sample size calculation was based on law of diminishing return ("resource equation" method), with a degree of freedom of analysis of variance of 19 [54]. After a satisfactory clinical inspection, the hamsters were housed in polycarbonate boxes 1264 C Eurostandard Type II, floor area 370 cm^2 (Tecniplast, Italy) at a rate of two animals *per* box at CICDC's facility. Cages were identified with the following information: species, sex, age, name of the project, group of randomization, number and physical mark for identification. The hamsters were used after one week of acclimatization.

Animals received sterile pelletized feed EMO-1002 (AlyCo®, CENPALAB, Havana, Cuba) and acidified water ad libitum. During the experimental phase, animals were kept in a CICDC Biosafety Laboratory Level 3 (BSL-3) with the required environmental conditions of temperature (20 ± 2 ºC), relative humidity between 50% and 60%, and with a 12 by 12 h light-dark cycle. All experiments with animals were carried out in conformity to the Directive 2010/63/EU of the European Parliament and of the European Union council (22 September 2010) on the protection of animals used for scientific purposes. All efforts were made to minimize animal suffering and to reduce the number of animals used. Animals were euthanized with an overdose of thiopental.

All work with viable SARS-CoV-2 was performed in BSL-3 facilities.

2.3. Antiviral assay on Vero E6

Vero E6 monolayers were inoculated with 100 $TCID_{50}$ of SARS-CoV-2 strain CUT-2010–2025 in 100 μL/well of supplemented MEM and incubated for 1 h. Then, cells were washed twice with phosphate-

buffered saline (PBS) solution at pH 7.3–7.5. Six different concentrations of lithium (Li^+), ranging 2–12 mmol/L, were prepared from a stock solution of LiCl*H_2O dissolved in MEM with 2% FBS. A volume of 100 μL/well of each concentration was added to Vero E6 monolayer using six replicates. Each assay plate contained cells, either inoculated or not, as viral or cellular controls, respectively.

Microplates were incubated for 96 h at 37ºC in 5% CO_2 atmosphere. Cytopathic effects were recorded 96 h after inoculation under inverted microscope. The antiviral efficacy of lithium was evaluated spectrophotometrically using the NR uptake assay [55] with slight modifications. Briefly, after removing the supernatant, 100 μL of 0.02% NR was added to each well. After incubating cells for 1 h at room temperature (20–25ºC) in the dark, NR solution was removed and cells were washed twice with 0.05% Tween-20 in PBS. A volume of 50 μL of lysis buffer (absolute ethanol/ultrapure water/glacial acetic acid, 50:49:1, v/v/v) *per* well was added, and plates were incubated for 15 min. Absorbance was measured using a PR621 microplate reader (Immunoassay Center, Havana, Cuba) at 520 nm [56].

Results were expressed as a percentage (%) of inhibition of lithium over SARS-CoV-2 replication. It was calculated using the following equation: $\%\ inhibition = 100\ [(As - Avc)/(Acc - Avc)]$, where *As* is the absorbance of the sample, *Avc* is the absorbance of the viral control, and *Acc* is the absorbance of the cellular control. Half-maximal inhibitory concentration (IC_{50}) is the most widely used and informative measure of a drug's efficacy and indicates how much drug is needed to inhibit a biological process by half. Lithium half-maximal inhibitory concentration was defined as the concentration which achieved 50% inhibition of virus-induced cytopathic effects and was determined through a non-linear regression analysis of the concentration-response curve on Fig. 3, using GraphPad Prism 8.0 software (GraphPad Inc., CA, USA) [57].

After visualizing the cytopathic effect, the supernatants were collected to detect and compare the amount of viral proteins. A standardized sandwich ELISA was performed in polypropylene 96-well plates, coated with 10 μg/mL of CBSS NCoV for capture. Sensitization was performed in a humid chamber at 37ºC for 2 h, with 100 μL/well of Na_2CO_3-$NaHCO_3$ (0.05 mol/L, pH 9.6). Plates were washed four times with BSS-Tween 20 1X that contains NaH_2PO_4 (0.6 g/L), NaCl (4 g/L), KCl (0.2 g/L) and Na_2HPO_4 * 12 H_2O (1.9 g/L) at pH of 7.2–7.4% and 0.31% of Tween-20. Plates were blocked with BSA and dried at room temperature for 24 h.

N protein of SARS-CoV-2 was used as positive control. The supernatant of non-infected Vero E6 was used as negative control. BSS that contains NaCl (100 g/L), NaH_2PO_4 (15 g/L), KCl (5 g/L) and Na_2HPO_4 * 12 H_2O (47.5 g/L) with 1.25% of BSS-Tween-20 was used as a washing solution. CBSS NCoV conjugated to horseradish peroxidase was used for detection. TMB at 1:100 was used as chromogenic substrate.

Six replicates of samples were added to plates (100 μL /well) and incubated for 24 h at 37 °C in the dark in humid chamber. Plates were washed three times. Peroxidase conjugate was added to wells followed by incubation at 37 °C for 1 h in the dark, and then plates were washed. Revealing reaction was performed by adding 100 μL of TMB and incubating for 20 min. Reaction was stopped with 50 μL/well of a 4 mol/L sulfuric acid solution. Absorbance was measured using a PR621 reader at 450 nm. Cut-off value was established as the mean of the OD values of the negative controls plus three standard deviations (SDs). Samples with an absorbance value greater than or equal to the cut-off value were considered positive for the test.

Toxicity controls were set up in parallel on uninfected cells in every experiment.

2.4. Syrian hamsters and lithium carbonate administration

Animals were randomized into five groups: negative and positive controls (n = 4 each); lithium control (n = 4); and two groups of infected animals treated with lithium, one on the same day of the infection (T-0) and the other on the day before (T-1) (n = 6 each).

Lithium carbonate was administrated daily, intragastrically, at 15 mg/Kg of weight in 200 μL of saline solution to all animals, except those in control groups who received 200 μL of intragastric saline. The determination of lithium in the serum of treated hamsters was performed using a Roche/Hitachi Cobas C system (Cobas 6000). The blood samples were allowed to clot, and the sera were separated by centrifugation at 3000 rpm for 5 min and stored at − 20 °C until the analysis was performed. Lithium-control animals were checked daily for any signs suggestive of toxicity. Studied signs were lethargy/inactivity, seizures, and gastrointestinal signs (diarrhea).

Hamsters were anesthetized using a ketamine/xylazine cocktail and inoculated via intranasal instillation of 100 $TCID_{50}$ of SARS-CoV-2 in 50 μL (25 μL in each nostril). Signs of the disease were monitored daily for all animals. Studied signs were lethargy, stooping and polypnea/abdominal breathing. Lethargy was defined as a clear state of reduced responsiveness and spontaneous activity; stooping was determined when the animal moved with hunched back or rested upright with the back hunched. To simplify the analysis of these signs, a value of one point was assigned to each of the signs observed *per* animal *per* day, making a maximum of three points *per* animal *per* day (lethargy, stooping and polypnea/abdominal breathing). Every animal was placed into an individual cage for 3 min. During this time, an observer blinded to the experimental conditions of the study, scored the hamsters according to the presence (=1) or absence (=0) of the evaluated sign (Fig. 5). All data were collected by observers blinded to the protocol.

Two animals of each group were euthanized on the fifth day post-infection. Nasal swabs followed by reverse transcriptase-polymerase chain reaction (RT-PCR) and culture on Vero E6 cells on days 2, 4, 5, and 7 were performed. The presence of the virus in the nasopharynx and lungs was determined. A histopathologic study of the lungs tissue was carried out. The left lung was fixed in 10% formalin before paraffin embedding. Tissue Section (3 μm) were analyzed after staining with hematoxylin and eosin (H:E) and scored blindly for lung damage by an expert pathologist. To facilitate the analysis, a value between 0 and 4 points was assigned to lung injure.

2.5. Statistical analyses

Statistical analysis was performed in GraphPad Prism 8.0 software (GraphPad Inc., CA, USA). Six replicates of all cells experiments were made and results were reported as the mean ± SD. T-tests were used to assess studies with two groups, and ANOVA was used to analyze studies with > 2 groups. A statistical significance was considered present when $p < 0.05$.

3. Results

3.1. Lithium treatment directly inhibits SARS-CoV-2 replication on Vero E6

Initially, to examine the effect of lithium salts on SARS-CoV-2, Vero E6 cells were cultured as monolayers in the presence or absence of lithium chloride monohydrate. Cells treated with lithium showed a significantly less cytopathic effect and more cellular viability than viral controls, as determined by inverted microscopic observation (Fig. 1) and NR uptake assay (Fig. 2), respectively. Maximal expression of cytopathic effect was detected on viral control wells at 96 h after inoculation. Cytopathic effect was characterized by cell monolayer destruction, with blank spaces, multinucleated giant cell (syncytium) formation, and cell rounding. Lithium-treated wells showed a significantly higher percentage of monolayer conservation than viral control, particularly at concentrations higher than 6 mmol/L (Fig. 1).

To further confirm the efficacy of lithium inhibition of SARS-CoV-2 replication in Vero E6 cells, an ELISA was performed to detect viral N protein in the harvested supernatant of a reduced sample of wells and

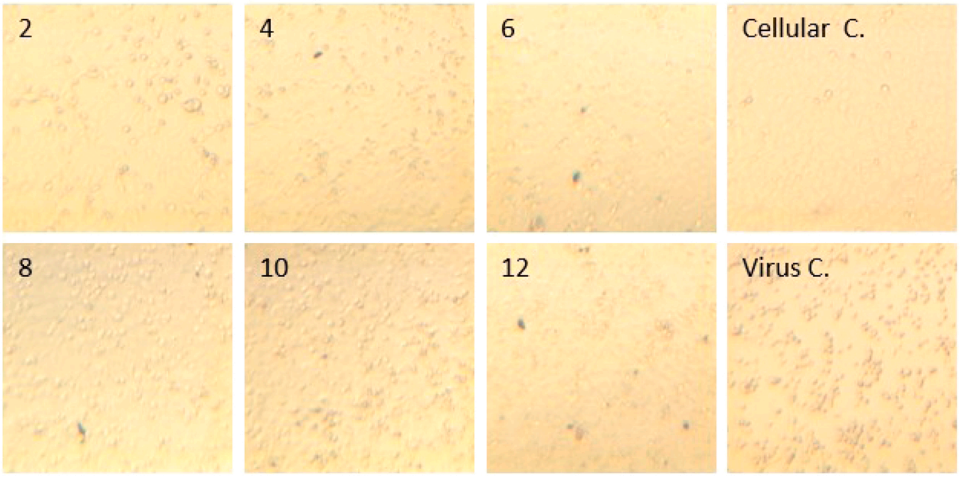

Fig. 1. Inverted microscope (100x) observation of the cytopathic effect of SARS-CoV-2 on Vero E6 monolayer treated with different concentrations of lithium (mmol/L) Legend: Numbers in the upper left corner of each photo indicate the lithium concentration in mmol/L; Cellular C. is the Vero E6 monolayer cultured under normal conditions; Virus C. is the Vero E6 monolayer infected with 100 TCID of SARS-CoV-2.

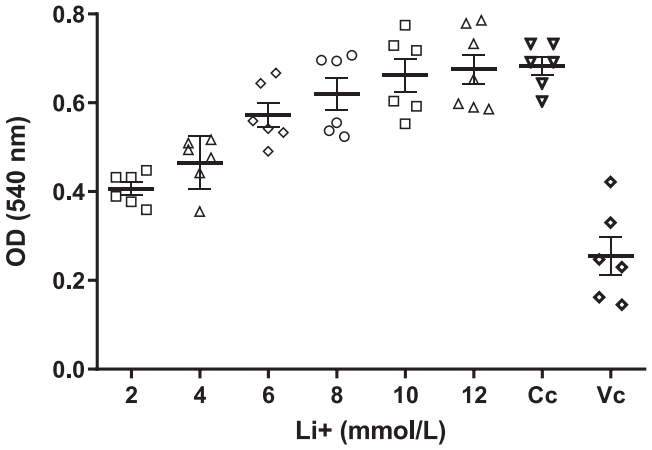

Fig. 2. Neutral red uptake assay in Vero E6 cells infected with SARS-CoV-2, treated with different concentrations of lithium (mmol/L) Legend: NR absorption expressed as optical density (OD) correlates with cellular viability. Infected-treated wells under increasing concentrations of lithium are shown. Cc represents the cellular control; Vc represents the viral control (infected-untreated). Absorbance was measured using a PR621 reader at 540 nm. Error bars represent the standard error of the mean (SEM). Lithium inhibited the replication of SARS-CoV-2 virus in a dose-dependent manner with an IC_{50} value of 4 mmol/L (Fig. 3). Viability of non-infected Vero E6 cells in the presence of lithium are shown.

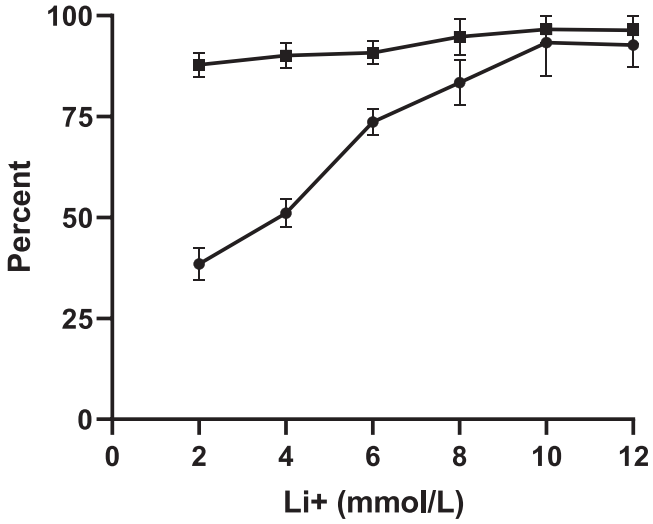

Fig. 3. Antiviral activity of lithium against SARS-CoV-2 virus in Vero E6 cells and viability of lithium-treated cells Legend: Percent of inhibition of SARS-CoV-2 replication in Vero E6 cells, under increasing concentrations of lithium, is represented with circles; black squares represent viability of lithium-treated cells. Absorbance was measured using a PR621 reader at 540 nm. Error bars represent the SEM.

not all lithium concentrations were evaluated. Determination of N protein in treated wells matched the uninfected cellular control observing a significant downgrading ($p < 0.001$). Fig. 4 represents the mean OD in the supernatant of treated cells, according to concentrations evaluated. This semi-quantitative method allowed us to compare concentrations of the N protein of SARS-CoV-2 in supernatants of treated and untreated infected-cells. Overall, direct anti-SARS-CoV-2 effect of lithium, evaluated by cytopathic effects, cell-viability and absence of viral replication was demonstrated.

3.2. Lithium treatment affects SARS-CoV-2 infection decreasing the appearance and intensity of signs of COVID-19 in Syrian hamsters

Clinical signs of COVID-19 were markedly reduced in both groups of Syrian hamsters treated with lithium. There were no significant differences between this groups and the signs of both were presented together in Fig. 5. Absence of signs prevailed in four animals, another four presented signs only for one day, one animal for two days, and none had polypnea. Meanwhile, all animals in the viral control group showed lethargy and stooping between days 3–5 post-infection, and two of them had polypnea on the fifth day (Table 1). Three animals died after anesthesia on the first day (two in T-1 and one in T-0) and were excluded from statistical analysis.

No signs of the disease were found in animals of negative control group (Fig. 5). No lithium-related mortality or overt signs of toxicity were observed during the experiment. Loss of weight with referred infective dose was not observed (data not shown).

In the histopathological evaluation of the lungs five days after infection, large leukocyte condensates were observed with loss of normal histology of the organ of the infected-untreated controls, with a high percentage of lung involvement. Animals treated with lithium were characterized by small inflammatory condensates and peribronchiolar infiltrates (Fig. 6), which, according to clinical manifestations, did not

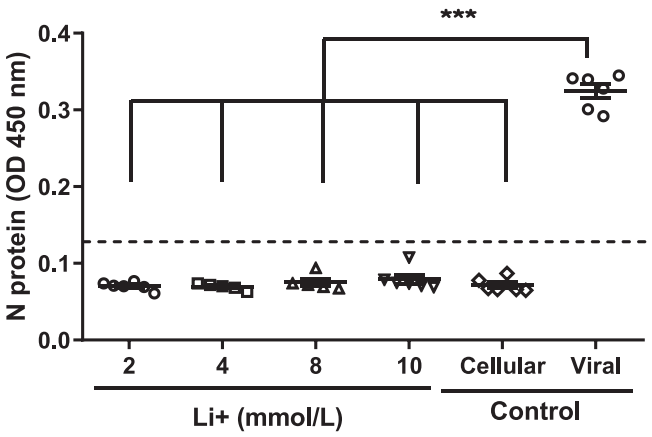

Fig. 4. Concentration of N protein of SARS-CoV-2 in the supernatant of culture Vero E6 treated with lithium. Legend: A standardized sandwich ELISA was performed to determine the N protein of SARS-CoV-2 in the harvested supernatant of treated wells. Absorbance was measured using a PR621 reader at 450 nm. Cut off value was set up at 0.129.

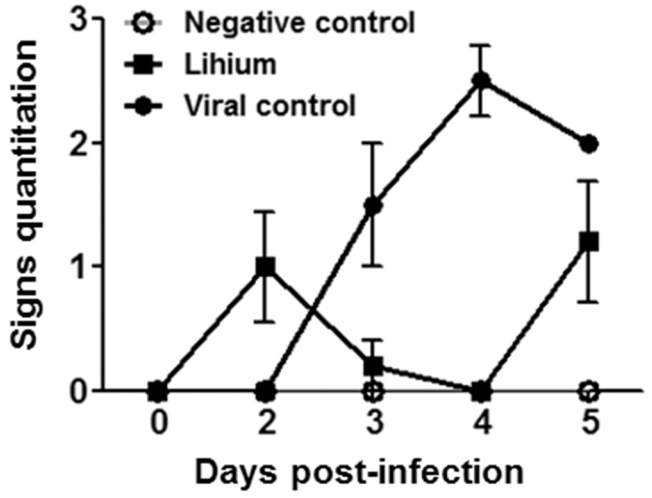

Fig. 5. Assessment of COVID-19 signs in SARS-CoV-2-infected hamsters Legend: Mean and error of cumulative signs for each group. Black squares represent infected hamsters treated with lithium (T-1 and T-0 groups were combined); black circles represent infected untreated hamsters. Error bars represent the SEM.

have great repercussions on the dynamics of the organism. An inflammatory condensate of large magnitude was observed only in one treated animal (Table 1).

Samples obtained by nasopharyngeal swab, nasopharyngeal lavage, or lung maceration after euthanasia were seeded in Vero E6 cell cultures to confirm the infection. A RT-PCR was also performed to compare the viral load in each animal. Between days 2 and 4 post-infection, there was a trend towards a lower viral load (higher Ct value including three with a value higher than 35, considering negative at day 4) in hamsters treated with lithium over viral controls. This was also observed in the analysis of the lungs of euthanized hamsters on the fifth day post-infection. However, an inconclusive dispersion was observed in terms of viral load of swabbing and nasopharyngeal lavages on the fifth day post-infection (Fig. 7). In our study, the intensity of clinical signs of COVID-19 in Syrian hamsters did not directly correlate with the viral load detected in each animal. At 11 days, all animals became negative by RT-PCR (data not shown). Overall, the effects of lithium on SARS-CoV-2 infection in hamsters, particularly at signs and lungs histology levels (regarding signs and lung injure), were demonstrated.

4. Discussion

SARS-CoV-2 causes a severe respiratory disease (COVID-19) that remains a global crisis [1]. Any new therapeutic approaches will be of importance and potentially could save lives. In this paper, we provide evidence that lithium salts have ablative effects in vitro on the infection of cells and in a Syrian hamster model of infection. We found that lithium inhibited the replication of SARS-CoV-2 in Vero E6 cells in a concentration-dependent manner. The Vero E6 monolayer was conserved as verified by microscopic observation and a NR uptake assay. Cell viability is directly proportional to NR absorption. Fig. 2 clearly shows a superior uptake of NR (expressed as OD) of lithium-treated wells compared to the viral control (infected-untreated). This is consistent with an important antiviral effect of lithium, as show in Fig. 3. Further, using an ELISA we showed that lithium effectively reduced viral titers when comparing the OD of the supernatants of treated wells with the OD of the supernatants of viral control cells ($p < 0.001$).

Previous studies have shown that lithium salts can reduce coronaviruses infection when used at concentrations ranging from 5 to 25 mmol/L [31,33,58,59]. Tested concentrations in our study correlates with antiviral evaluation led by Harrison et al. on the avian coronavirus infectious bronchitis virus, a work that demonstrated that 5 mmol/L of LiCl cause a 50% reduction in virus titers [33]. Liu et al. [10] showed that GSK-3 inhibitors, including lithium, inhibit SARS-CoV-2 N protein phosphorylation, an essential step in viral replication. LiCl inhibited N phosphorylation with IC_{50} ~10 mM in 293 T cells, above the concentration needed to inhibit viral replication in Vero E6 cells in our study. Liu et al. also demonstrated that low doses of the highly selective GSK-3 inhibitor CHIR99021 reduced viral titers over 15-fold in the supernatant from SARS-CoV-2–infected human lung epithelium-derived cell line Calu-3.

Our findings are consistent with and supported by the recent in vitro studies of Shapira et al. [60], who tested three active compounds with GSK3β inhibitory effects and demonstrated their ability to reduce SARS-CoV-2 infection in various cell lines, with a significant 2-log reduction 48 h after infection and treatment.

In vitro non-toxic concentrations of lithium chloride have been set up between 15 and 50 mmol/L [31,58,59]. Our study evaluated concentrations up to 12 mmol/L of Li^+. Although we did not perform a full toxicity assay, we assessed the non-toxicity of used concentrations in parallel.

As coronaviruses require host GSK-3 activity for their replication [10,19], its inhibition represents a direct antiviral mechanism of lithium. Besides, lithium can potentiate CTL activity through PD-1 and LAG3 inhibition, favoring indirect antiviral activity. Although it is difficult to translate pre-clinical results into actual clinical treatment in patients, lithium has advantages over other antiviral drugs. In addition to its antiviral activity, lithium has anti-inflammatory effects by decreasing the production/expression of inflammatory-associated mediators [37] such as prostaglandin E_2, cyclooxygenase-2 [61] and various pro-inflammatory cytokines, including interleukin (IL) 1 [39], IL-6 [39,62] and tumor necrosis factor-alpha (TNF-α) [63].

With these results on cellular cultures, we decided to assess the therapeutic effect and safety of lithium on Syrian hamsters infected with SARS-CoV-2. It was determined to use 100 $TCID_{50}$ as infective dose that is 20 times higher than the average infective dose of SARS-CoV-2 for this animal model [47]. This allowed us to observe the appearance of a moderate/severe disease in these animals. As the most frequent signs of COVID-19 described in Syrian hamsters are loss of weight, stooping, lethargy and polypnea [47,49–51], it was decided to evaluate them on a daily basis. Surprisingly, no significant loss of weight was observed in infected animals. This may be due to the low infective dose used compared to other studies [47,49–51]. We hypothesized that the higher the infective dose, the greater the weight loss. We found that hamsters treated with lithium showed a less intense disease with fewer signs. Some animals treated with lithium did not show any signs of the disease.

Table 1
COVID-19 behavior in Syrian hamsters treated or not with lithium carbonate.

Group	No	Signs (days)												Histol. 5 PI
		2			3			4			5			
		L	S	P	L	S	P	L	S	P	L	S	P	Lungs
T-1	9	0	0	0	0	0	0	0	0	0	2	2	0	3
	11	2	2	0	0	0	0	0	0	0	2	2	0	1
	12	2	2	0	0	0	0	0	0	0	0	0	0	Nd
	13	0	0	0	0	0	0	0	0	0	0	0	0	Nd
T-0	15	0	0	0	0	0	0	0	0	0	0	0	0	1
	16	0	0	0	0	0	0	0	0	0	0	0	0	1
	18	0	0	0	0	0	0	0	0	0	0	0	0	Nd
	19	0	0	0	0	0	0	0	0	0	2	2	0	Nd
	20	0	0	0	0	0	0	0	0	0	2	2	0	Nd
C+	21	0	0	0	2	2	0	4	4	4	2	2	0	3.5
	22	0	0	0	2	2	0	2	2	0	2	2	0	2.5
	23	0	0	0	0	0	0	2	2	0	2	2	0	Nd
	24	0	0	0	2	2	0	4	4	4	2	2	0	Nd

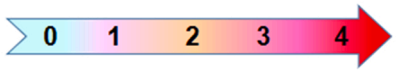

Legend: C+ represents the positive control (infected-untreated); T-0 represents infected-treated with lithium starting on the same day of the infection; T-1 represents infected-treated with lithium starting on the day before the infection. The arrow represents gradation of the intensity of signs, from absence to maximum intensity. L, lethargy; S, stooping; P, polypnea; PI, days post-infection; Nd, not done.

The presence of signs in the viral control group (infected untreated) was significantly higher than those treated with lithium. This is more evident in Fig. 5, since although the n in the groups treated with lithium was significantly higher (n = 9) than in the untreated group (n = 4), the average number of signs of hamsters *per* day, was higher in the group of the infected-untreated animals. Even two animals of the viral control group showed polypnea, a sign that reflects the greater severity of the disease.

As a worsening peak has been described on the fifth day post-infection in this animal model, followed by rapid improvement [50], it was therefore decided to euthanize two animals in each group to compare the viral load and histological lesions in the lungs.

We evaluated in vivo the antiviral and immunotherapeutic potential of lithium. Despite the fact that between days 2 and 4 post-infection a trend towards a decrease in viral load was observed in treated hamsters compared to controls, on the fifth day post-infection an inconclusive dispersion was noted in the Ct value of the swab and nasopharyngeal lavage samples. However, viral load in lungs at fifth day post-infection was also discreetly inferior in treated animals.

Finally, the histopathologic study of the lungs showed less tissue damage in those treated animals compared to the untreated ones, which is consistent with the decreased amount of signs of the disease found in the study group. Given that the freedom of analysis in this case [54] was below 10, these findings should be interpreted carefully and further investigations are required with larger sample size.

The assessment of the immunotherapeutic effect of lithium salts in animal models allows us not only to evaluate their antiviral capacity, but also other properties such its immune-potentiating and anti-inflammatory effects.

Due to the rapid evolution of the disease in Syrian hamsters and the high replication rate of SARS-CoV-2 in this animal model [49,50], we decided to explore whether there were differences between hamsters treated 24 h before infection in comparison to those that started treatment the same day of infection. There were no significant differences between the groups treated with lithium. This may be due to the rapid intestinal absorption of lithium [34] that does not require starting treatment from a day before in this animal model.

Unlike other drugs that did not replicate in Syrian hamsters the antiviral results obtained in cell cultures [64,65], lithium showed, although slight, a tendency to decrease the viral load in nasopharyngeal swabs and lungs. Although it must be said that the infective dose used in those studies was higher than ours, it has been shown that a low-dose challenge inoculum induced a comparable viral load and disease pathology compared with higher viral dose challenges [66].

A dose of 15 mg/kg of body weight of lithium carbonate *per* day was chosen for treatment. This dosing regime is equivalent to the usual daily dose in humans, about 1000 mg/day [34] and it yielded a serum lithium level of 0.91 ± 0.27 mmol/L, within the human therapeutic range. Hence, the data obtained from the current study could be extrapolated to clinical scenarios. For estimation of the toxicity of a drug, the mean lethal dose (LD50) is a commonly used pharmacological parameter and is determined in laboratory animals, preferably in mice and rats. For lithium carbonate the LD50 in rats is ~700 mg/kg after oral administration [67]. In our search we did not find the LD50 for Syrian hamsters and its determination is beyond the scope of this work. The lithium regimen used is markedly below the LD50 for lithium application in rats, and also below the usual doses in pre-clinical toxicology studies [68,69].

Taking into account the pre-clinical results shown here, it seems that the immunomodulatory/anti-inflammatory properties of lithium play a greater role in the improvement of subjects affected by COVID-19. This gains relevance as the inflammatory host response drives much of the pathology of the SARS CoV-2 infection. A reduced incidence of COVID-19 in patients taking lithium compared to the general population was demonstrated after the analysis of clinical data from four major health systems [10,40]. Unfortunately, severity and mortality data were not obtained and compared between the two groups of infected patients, since modulation of the inflammatory response by lithium may also contribute to reduce the risk of COVID-19 severity and mortality [70].

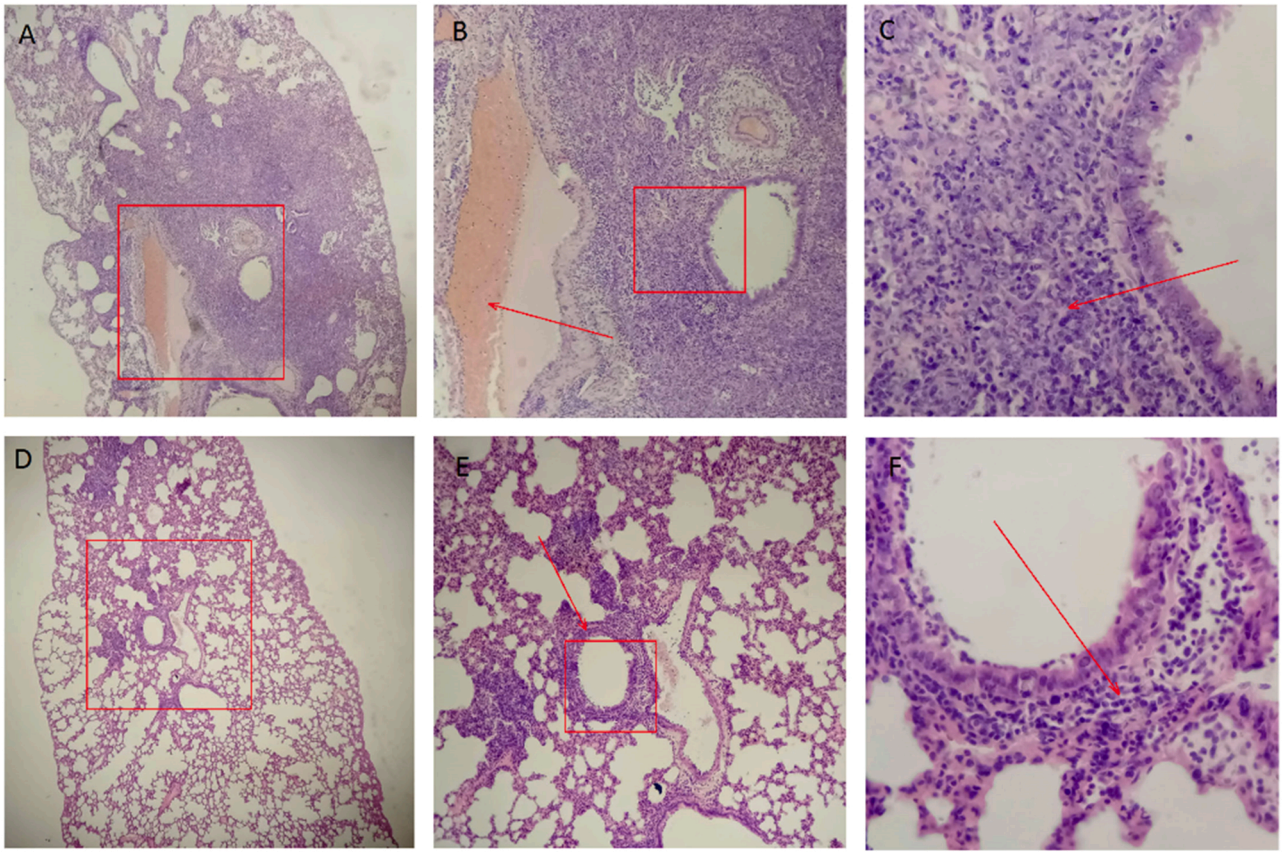

Fig. 6. Histopathologic study of the lungs tissue of infected Syrian hamsters Legend: Tissue Section (3 μm) staining with hematoxylin and eosin A-C. Infected-untreated hamster (40x-400x): large leukocyte condensates, high percentage of lung injury; D-F: infected-treated with lithium (40x-400x), smaller inflammatory condensates and peribronchiolar infiltrates.

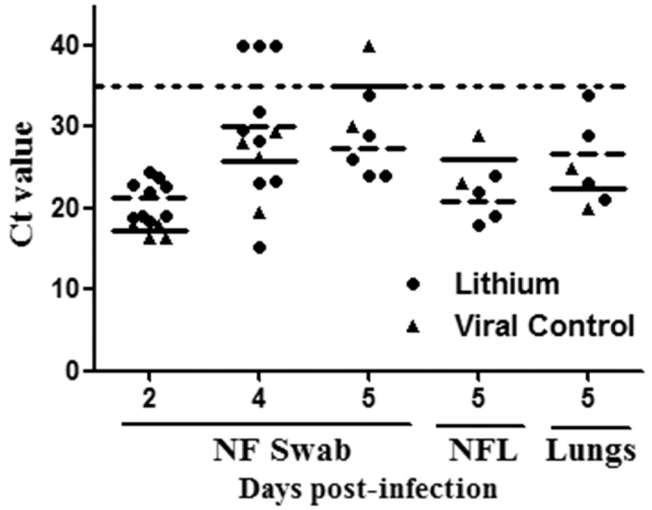

Fig. 7. RT-PCR for SARS-CoV-2 in infected Syrian hamsters Legend: NF, nasopharyngeal; NFL, NF lavage. Horizontal lines represent the mean of each group (continuous for viral control; discontinuous for lithium-treated). Cut off value of Ct was established at 35.

Spuch et al. [40] treated six patients with severe COVID-19 with lithium carbonate. The authors found that lithium carbonate reduced plasma C-reactive protein levels and increased lymphocyte numbers, reducing the neutrophil-lymphocyte ratio. All patients treated with lithium carbonate improved their clinical status and no side effects related to lithium carbonate treatment were reported. These preliminary data suggest that lithium treatment reduces the inflammatory state of patients with COVID-19, improving both inflammatory activity and the immune response. Because of the limitations of this study such as the small number of cases and the lack of randomization, these findings should be interpreted carefully and deeper investigation is required in a cohort with larger sample size.

Four cases of lithium toxicity in COVID-19 patients under long-term lithium treatment have been reported [71,72]. A recent study stablished a 1% incidence of lithium intoxication in chronically treated patients [73]. They assessed the incidence, clinical course and renal function based in a retrospective cohort study, and concluded that lithium intoxication seems rare and can be safely managed in most cases. Also, lithium intoxication is associated with prolonged use, and short period treatment could minimize the events associated with toxicity [74].

Considering the world's current situation as a consequence of the SARS-CoV-2 pandemic, we believe that the information provided by this study supports the performance of clinical trials for the lithium treatment of patients with COVID-19.

4.1. Limitations of study

Our study has the limitation of have not determined pro-inflammatory markers (i.e. C-reactive protein and IL-6) in Syrian hamsters treated or not with lithium.

5. Conclusions

Lithium directly inhibits the replication of SARS-CoV-2 in Vero E6 cells in a concentration-dependent manner. It was effective in treating Syrian hamsters with COVID-19, evidenced by a decrease in viral load

and the appearance of signs of the disease and/or its intensity. These results reaffirm the possible therapeutic effect of lithium salts and support further clinical trials in patients with COVID-19.

Authors contributions

OP, OST, and ENR designed and led the study.ENR, OST, NGS, ROH, JMEP, MGM, AFQ, YIH, DMA, MTZD and IAH performed the virological assays and experimental work, and contributed to analysis of the results and preparation of figures. ML, LRP, RRP, LMR, IGV, VEG, MRA, IGR, AMS, LAC and YB supported and contributed to the study design and analysis. All authors revised the manuscript and approved submission.

Ethics statement

Animal experimental procedures were approved by the Ethics Committee of CICDC and performed in compliance with national and international guidelines for care and humane use of animals, and in conformity to the Directive 2010/63/EU of the European Parliament and of the European Union council (22 September 2010) on the protection of animals used for scientific purposes.

Conflict of interest statement

The authors declare no conflict of interest.

Data availability

Data will be made available on request.

Acknowledgments

The authors are indebted to CICDC staff for their collaborative support and dedication during the experiments. We are grateful to YJ González for her technical support, constructive discussions, and scientific input. We also thank J Delgado and SR Páez from Empresa Central de Laboratorios “José Isaac del Corral”, Havana, Cuba, for their invaluable contribution. We also thank JF Infante for the anatomopathological evaluation of hamsters. CE Rudd is supported by a grant from the Canadian Institutes of Health Research (CIHR).

References

[1] C. Huang, Y. Wang, X. Li, L. Ren, J. Zhao, Y. Hu, et al., Clinical features of patients infected with 2019 novel coronavirus in Wuhan, China, Lancet 395 (2020) 497–506, https://doi.org/10.1016/S0140-6736(20)30183-5.
[2] J.F.W. Chan, K.H. Kok, Z. Zhu, H. Chu, K.K.W. To, S. Yuan, et al., Genomic characterization of the 2019 novel human-pathogenic coronavirus isolated from a patient with atypical pneumonia after visiting Wuhan, Emerg. Microbes Infect. 9 (1) (2020) 221–236, https://doi.org/10.1080/22221751.2020.1719902.
[3] P.A. Rota, M.S. Oberste, S.S. Monroe, W.A. Nix, Characterization of a novel coronavirus associated with severe acute respiratory syndrome, Science 300 (2003) 1394–1399.
[4] R. Lu, X. Zhao, J. Li, P. Niu, B. Yang, H. Wu, et al., Genomic characterisation and epidemiology of 2019 novel coronavirus: implications for virus origins and receptor binding, Lancet (2020) 395, 565e74.
[5] C. Wu, Y. Liu, Y. Yang, P. Zhang, W. Zhong, Y. Wang, Analysis of therapeutic targets for SARS-CoV-2 and discovery of potential drugs by computational methods, Acta Pharm. Sin. B 10 (766–88) (2020), https://doi.org/10.1016/j.apsb.2020.02.008.
[6] C.R. Carlson, J.B. Asfaha, C.M. Ghent, C.J. Howard, N. Hartooni, M. Safari, et al., Phosphoregulation of phase separation by the SARS-CoV-2 N protein suggests a biophysical basis for its dual functions, Mol. Cell 80 (2020) 1092–1103, https://doi.org/10.1016/j.molcel.2020.11.025.
[7] T.M. Perdikari, A.C. Murthy, V.H. Ryan, S. Watters, M.T. Naik, N.L. Fawzi, SARS-CoV-2 nucleocapsid protein phase-separates with RNA and with human hnRNPs, EMBO J. 39 (2020), e106478, https://doi.org/10.15252/embj.2020106478.
[8] C.-K. Chang, M.-H. Hou, C.-F. Chang, C.-D. Hsiao, T.-H. Huang, The SARS coronavirus nucleocapsid protein – forms and functions, Antivir. Res. 103 (2014) 39–50, https://doi.org/10.1016/j.antiviral.2013.12.009.
[9] C.H. Wu, P.J. Chen, S.H. Yeh, Nucleocapsid phosphorylation and RNA helicase DDX1 recruitment enables coronavirus transition from discontinuous to continuous transcription, Cell Host Microbe 16 (4) (2014) 462–472, https://doi.org/10.1016/j.chom.2014.09.009.
[10] X. Liu, A. Verma, J. Garcia, H. Ramage, A. Lucas, R.L. Myers, et al., Targeting the coronavirus nucleocapsid protein through GSK-3 inhibition, Proc. Nat. Acad. Sci. 118 (42) (2021), https://doi.org/10.1073/pnas.2113401118.
[11] O. Kaidanovich-Beilin, J. Robert Woodgett, GSK-3: functional insights from cell biology and animal models, Front Mol. NeuroSci. 4 (2011) 40, https://doi.org/10.3389/fnmol.2011.00040.
[12] E. Beurel, S.F. Grieco, R. Jope, Glycogen synthase kinase-3 (GSK3): regulation, actions, and diseases, Pharmacol. Ther. 148 (2015) 114–131, https://doi.org/10.1016/j.pharmthera.2014.11.016.
[13] A. Taylor, J.A. Harker, K. Chanthong, P.G. Stevenson, E.I. Zuniga, C.E. Rudd, Glycogen synthase kinase 3 inactivation drives T-bet-mediated downregulation of co-receptor PD-1 to enhance CD8+ cytolytic T cell responses, Immunity 44 (2016) 274–286, https://doi.org/10.1016/j.immuni.2016.01.018.
[14] Y. Agata, A. Kawasaki, H. Nishimura, Y. Ishida, T. Tsubata, H. Yagita, et al., Expression of the PD-1 antigen on the surface of stimulated mouse T and B lymphocytes, Int Immunol. 8 (1996) 765–772.
[15] S. Gordon, R.L. Maute, B.W. Dulken, G. Hutter, B.M. George, M.N. McCrcken, et al., PD-1 expression by tumor-associated macrophages inhibits phagocytosis and tumor immunity, Nature 545 (7655) (2017) 495–499, https://doi.org/10.1038nature22396.
[16] C. Niu, M. Li, S. Zhu, Y. Chen, L. Zhou, D. Xu, et al., PD-1-positive natural killer cells have a weaker antitumor function than that of PD-1-negative Natural Killer Cells in Lung Cancer, Int J. Med Sci. 17 (13) (2020) 1964–1973, https://doi.org/10.7150/ijms.47701.
[17] T.S. Lim, V. Chew, J.L. Sieow, S. Goh, J.P.-S. Yeong, A.L. Soon, et al., PD-1 expression on dendritic cells suppresses CD8+T cell function and antitumor immunity, OncoImmunology 5 (3) (2016), e1085146, https://doi.org/10.1080/2162402X.2015.1085146.
[18] L. Skalniak, K.M. Zak, K. Guzik, K. Magiera, B. Musielak, M. Pachota, et al., Small-molecule inhibitors of PD-1/PD-L1 immune checkpoint alleviate the PD-L1-induced exhaustion of T-cells, Oncotarget 8 (42) (2017) 72167–72181, https://doi.org/10.18632/oncotarget.20050.
[19] P.S. Chowdhury, K. Chamoto, T. Honjo, Combination therapy strategies for improving PD-1 blockade efficacy: a new era in cancer immunotherapy, J. Intern Med 283 (2) (2018) 110–120, https://doi.org/10.1111/joim.12708.
[20] M. Reck, D. Rodriguez-Abreu, A.G. Robinson, Pembrolizumab versus chemotherapy for PD-L1-positive non-small-cell lung cancer, N. Engl. J. Med 375 (19) (2016) 1823–1833, https://doi.org/10.1056/NEJMoal1606774.
[21] C.E. Rudd, K. Chanthong, A. Taylor, Small molecule inhibition of GSK-3 specifically inhibits the transcription of inhibitory co-receptor LAG-3 for enhanced anti-tumor immunity, e4, Cell Rep. 30 (7) (2020) 2075–2082, https://doi.org/10.1016/j.celrep.2020.01.076.
[22] T. Maruhashi, D. Sugiura, Okazaki I-m, T. Okazaki, LAG-3: from molecular functions to clinical applications, J. Immunother. Cancer 8 (2) (2020), https://doi.org/10.1136/jitc-2020-001014.
[23] P.S. Klein, D.A. Melton, A molecular mechanism for the effect of lithium on development, Proc. Nat. Acad. Sci. 93 (16) (1996) 8455–8459. ⟨https://www.pnas.org/content/pnas/93/16/8455.full.pdf⟩.
[24] F. López-Muñoz W., W. Shen, P. DOcon, A history of the pharmacological treatment of bipolar disorder, Int J. Mol. Sci. 19 (2018) 2143, https://doi.org/10.3390/ijms19072143.
[25] G.R. Skinner, C. Hartley, A. Buchan, L. Harper, P. Gallimore, The effect of lithium chloride on the replication of herpes simplex virus, Med Microbiol Immunol. 168 (2) (1980) 139–148, https://doi.org/10.1007/bf02121762.
[26] A. Murru, M. Manchia, T. Hajek, R.E. Nielsen, J.K. Rybakowski, G. Sani, et al., Lithium’s antiviral effects: a potential drug for CoViD-19 disease? Int J. Bipolar Disord. 8 (1) (2020) 1–9, https://doi.org/10.1186/s40345-020-00191-4.
[27] S.M. Harrison, I. Tarpey, L. Rothwell, P. Kaiser, J.A. Hiscox, Lithium chloride inhibits the coronavirus infectious bronchitis virus in cell culture, Avian Pathol. 36 (2) (2007) 109–114, https://doi.org/10.1080/03079450601156083.
[28] F.R. Zhao, Y.L. Xie, Z.Z. Liu, Lithium chloride inhibits early stages of foot-and-mouth disease virus (FMDV) replication in vitro, J. Med Virol. 89 (11) (2017) 2041–2046, https://doi.org/10.1002/jmv.24821.
[29] Y. Zhao, K. Yan, Y. Wang, J. Cai, L. Wei, S. Li, et al., Lithium chloride confers protection against viral myocarditis via suppression of coxsackievirus B3 virus replication, Micro Pathog. 144 (2020), 104169, https://doi.org/10.1016/j.micpath.2020.104169.
[30] M.A. Sarhan, M.S. Abdel-Hakeem, A.L. Mason, Glycogen synthase kinase 3beta inhibitors prevent hepatitis C virus release/assembly through perturbation of lipid metabolism, Sci. Rep. 7 (1) (2017) 2495, https://doi.org/10.1038/s41598-017-02648-6.
[31] H.-j Li, D.-s Gao, Y.-t Li, Y.-s Wang, H.-y Liu, J. Zhao, Antiviral effect of lithium chloride on porcine epidemic diarrhea virus in vitro, Res Vet. Sci. 118 (2018) 288–294, https://doi.org/10.1016/j.rvsc.2018.03.002.
[32] J.K. Nowak, J. Walkoviak, Lithium and coronaviral infections. A scoping review, F1000 Res. 9 (2020) 93, https://doi.org/10.12688/f1000research.22299.2.
[33] S.M. Harrison, I. Tarpey, L. Rothwell, P. Kaiser, J.A. Hiscox, Lithium chloride inhibits the coronavirus infectious bronchitis virus in cell culture, Avian Pathol. 36 (2) (2007) 109–114, https://doi.org/10.1080/03079450601156083.
[34] B. Medic, M. Stojanovic, B.V. Stimec, N. Divac, K.S. Vujovic, R. Stojanovic, et al., Lithium - pharmacological and toxicological aspects: the current state of the art, Curr. Med. Chem. 27 (3) (2020) 337–351, https://doi.org/10.2174/0929867325666180904124733.

[35] C. Yang, W. Wang, K. Zh, W. Liu, Y. Luo, X. Yuan, et al., Lithium chloride with immunomodulatory funtion for regulating titanium nanoparticle-stimulated inflammatory response and accelerating osteogenesis through suppression of MAPK signaling pathway, Int. J. Nanomed. 14 (2019) 7475–7488, https://doi.org/10.2147/IJN.S210834.
[36] M. Soares Fernandes, F. Barbisan, V. Farina Azzolin, P.A. Schmidt do Prado-Lima, C. Ferreira Teixeira, I.E. da Cruz Jung, et al., Lithium is able to minimize olanzapine oxidative-inflammatory induction on macrophage cells, PLoS ONE 14 (1) (2019), e0209223, https://doi.org/10.1371/journal.pone.0209223.
[37] A. Albayrak, Z. Halici, B. Polat, E. Karakus, E. Cadirci, Y. Bayir, et al., Protective effects of lithium: a new look at an old drug with potential antioxidative and anti-inflammatory effects in an animal model of sepsis, Int. Immunopharmacol. 16 (2013) 35–40.
[38] Y.J. Kwon, C.H. Yoon, S.W. Lee, Y.B. Park, S.K. Lee, M.C. Park, Inhibition of glycogen synthase kinase-3β suppresses inflammatory responses in rheumatoid arthritis fibroblast-like synovio-cytes and collagen-induced arthritis, Jt. Bone Spine (2013), https://doi.org/10.1016/j.jbspin.2013.09.006.
[39] E.M. Knijff, M.N. Breunis, R.W. Kupka, H.J. de Wit, C. Ruwhof, G.W. Akkerhuis, et al., An imbalance in the production of IL-1b and IL-6 by monocytes of bipolar patients: restoration by lithium treatment, Bipolar Disord. 9 (2007) 743–753.
[40] C. Spuch, M. López-García, T. Rivera-Baltanás, D. Rodrígues-Amorím, J. M. Olivares, Does lithium deserve a place in the treatment against COVID-19? a preliminary observational study in six patients, case report, Front Pharmacol. 11 (2020), 557629, https://doi.org/10.3389/fphar.2020.557629.
[41] N.S. Ogando, T.J. Dalebout, J.C. Zevenhoven-Dobbe, R.W.A.L. Limpens, Y. van der Meer, L. Caly, et al., SARS-coronavirus-2 replication in Vero E6 cells: replication kinetics, rapid adaptation and cytopathology, J. Gen. Virol. 101 (2020) 925–940, https://doi.org/10.1099/jgv.0.001453.
[42] E.C. Mossel, C. Huang, K. Narayanan, S. Makino, R.B. Tesh, J. Peters, Exogenous ACE2 expression allows refractory cell lines to support severe acute respiratory syndrome coronavirus replication, J. Virol. 79 (6) (2005) 3846–3850, https://doi.org/10.1128/JVI.79.6.3846-3850.2005.
[43] D.F. Barreto-Vieira, M.A. Nunes da Silva, C. Couto Garcia, M. Dias Miranda, A. da Rocha Matos, B. Costa Caetano, et al., Morphology and morphogenesis of SARS-CoV-2 in Vero-E6 cells, Mem. Inst. Oswaldo Cruz 116 (2021), e200443, https://doi.org/10.1590/0074-02760200443.
[44] D.F. Barreto-Vieira, M.A. Nunes da Silva, C.C. Garcia, M.D. Miranda, Ad.R. Matos, B.C. Caetano, et al., Morphology and morphogenesis of SARS-CoV-2 in Vero-E6 cells, Mem. Inst. Oswaldo Cruz 116 (e200443) (2021), https://doi.org/10.1590/0074-02760200443.
[45] S.R. Gong, L.L. Bao, The battle against SARS and MERS coronaviruses: reservoirs and animal models, Anim. Model Exp. Med. 1 (2) (2018) 125–133, https://doi.org/10.1002/ame2.12017.
[46] A. Roberts, L. Vogel, J. Guarner, N. Hayes, B. Murphy, S. Zaki, et al., Severe acute respiratory syndrome coronavirus infection of golden Syrian hamsters, J. Virol. 79 (1) (2005) 503–511, https://doi.org/10.1128/JVI.79.1.503-511.2005.
[47] K. Rosenke, K. Meade-White, M. Letko, C. Clancy, F. Hansen, Y. Liu, et al., Defining the Syrian hamster as a highly susceptible preclinical model for SARS-CoV-2 infection, Emerg. Microbes Infect. 9 (1) (2020) 2673–2684, https://doi.org/10.1080/22221751.2020.1858177.
[48] M. Imai, K. Iwatsuki-Horimoto, M. Hatta, S. Loeber, P.J. Halfmann, N. Nakajima, et al., Syrian hamsters as a small animal model for SARS-CoV-2 infection and countermeasure development, Proc. Natl. Acad. Sci. USA 117 (2020) 16587–16595.
[49] J.F. Chan, A.J. Zhang, S. Yuan, V.K. Poon, C.C.-S. Chan, A.C.-Y. Lee, et al., Simulation of the clinical and pathological manifestations of Coronavirus Disease 2019 (COVID-19) in golden Syrian hamster model: implications for disease pathogenesis and transmissibility, Clin. Infect. Dis. 71 (9) (2020) 2428–2446, https://doi.org/10.1093/cid/ciaa325.
[50] S.F. Sia, L.M. Yan, A.W.H. Chin, K. Fung, K.-T. Choy, A.Y.L. Wong, et al., Pathogenesis and transmission of SARS-CoV-2 in golden hamsters, Nature 583 (7818) (2020) 834–838, https://doi.org/10.1038/s41586-020-2342-5.
[51] A.C.-Y. Lee, A.J. Zhang, J.F.-W. Chan, J. Zhou, H. Chu, K.-Y. Yuen, et al., Oral SARS-CoV-2 inoculation establishes subclinical respiratory infection with virus shedding in golden syrian hamsters, Cell Rep. Med. 1 (7) (2020), 100121, https://doi.org/10.1016/j.xcrm.2020.100121.
[52] L.J. Reed, H. Muench, A simple method of estimating fifty percent endpoints, Am. J. Hyg. 27 (3) (1938) 493–497, https://doi.org/10.1093.oxfordjournals.aje.a118408.
[53] G. Álvarez, M. Dubed, E. Noa, L.M. Navea, M.T. Pérez, A. Rodríguez, Validación del método de titulación del virus de la inmunodeficiencia humana tipo 1, Rev. Cub Med Trop. 61 (2) (2009) 1–8.
[54] M.F. Festing, D.G. Altman, Guidelines for the design and statistical analysis of experiments using laboratory animals, ILAR J. 43 (4) (2002) 244–258, https://doi.org/10.1093/ilar.43.4.244.
[55] E. Borenfreund, J. Puerner, A simple quantitative procedure using monolayer cultures for cytotoxicity assays (HTD/NR90), J. Tissue Cult. Methods 9 (1) (1984) 7–9, https://doi.org/10.1007/BF01666038.
[56] A. Manenti, M. Maggetti, E. Casa, D. Martinuzzi, A. Torelli, C.M. Trombetta, et al., Evaluation of SARS-CoV-2 neutralizing antibodies using a CPE-based colorimetric live virus micro-neutralization assay in human serum samples, J. Med Virol. 92 (10) (2020) 2096–2104, https://doi.org/10.1002/jmv.25986.
[57] J. Sebaugh, Guidelines for accurate EC50/IC50 estimation, Pharm. Stat. 10 (2) (2011) 128–134, https://doi.org/10.1002/pst.426.
[58] L. Jing, Y. Jiechao, S. Xiuwen, L. Guangxing, R. Xiaofeng, Comparative analysis of the effect of glycyrrhizin diammonium and lithium chloride on infectious bronchitis virus infection in vitro, Avian Pathol. 38 (3) (2009) 215–221, https://doi.org/10.1080/03079450902912184.
[59] X. Ren, F. Meng, J. Yin, G. Li, X. Li, C. Wang, Action mechanisms of lithium chloride on cell infection by transmissible gastroenteritis coronavirus, PLoS ONE 6 (5) (2011), e18669, https://doi.org/10.1371/journal.pone.0018669.
[60] T. Shapira, C. Rens, V. Pichler, W. Rees, T. Steiner, F. Jean, et al., Inhibition of glycogen synthase kinase-3-beta (GSK3β) blocks nucleocapsid phosphorylation and SARS-CoV-2 replication, Res. Square (2022), https://doi.org/10.21203/rs.3.rs-1197371/v1. Preprint.
[61] F. Bosetti, J. Rintala, R. Seemann, T.A. Rosenberger, M.A. Contreras, S.I. Rapoport, et al., Chronic lithium downregulates cyclooxygenase-2 activity and prostaglandin E2 concentration in rat brain, Mol. Psych. 7 (2002) 845–850, https://doi.org/10.1038/sj.mp.4001111.
[62] B. Li, C. Zhang, F. He, W. Liu, Y. Yang, H. Liu, et al., GSK-3β inhibition attenuates LPS-induced death but aggravates radiation-induced death via down-regulation of IL-6, Cell Physiol. Biochem. 32 (2013) 1720–1728, https://doi.org/10.1159/000356606.
[63] A. Albayrak, Z. Halici, B. Polat, E. Karakus, E. Cadirci, Y. Bayir, et al., Protective effects of lithium: a new look at an old drug with potentialm antioxidative and anti-inflammatory effects in an animal model of sepsis, Int. Immunopharmacol. 16 (2013) 35–40, https://doi.org/10.1016/j.intimp.2013.03.018.
[64] Kaptein SJ, Jacobs S., Langendries L., Seldeslachts L., ter Horst S., Liesenborghs L., et al. Antiviral treatment of SARS-CoV-2-infected hamsters reveals a weak effect of favipiravir and a complete lack of effect for hydroxychloroquine. bioRxiv. 2020; Preprint. ⟨https://doi.org/10.1101/2020.06.19.159053⟩.
[65] Rosenke K., Jarvis MA, Feldmann F., Schwarz B., Okumura A., Lovaglio J., et al. Hydroxychloroquine Proves Ineffective in Hamsters and Macaques Infected with SARS-CoV-2. bioRxiv. 2020; Preprint. ⟨https://doi.org/10.1101/2020.06.10.145144⟩.
[66] J.E.M. van der Lubbe, S.K. Rosendahl Huber, A. Vijayan, L. Dekking, E. van Huizen, J. Vreugdenhil, et al., Ad26.COV2.S protects Syrian hamsters against G614 spike variant SARS-CoV-2 and does not enhance respiratory disease, npj Vaccin. 6 (2021) 39, https://doi.org/10.1038/s41541-021-00301-y.
[67] K.P. Petersen, Effect of age and route of administration on LD50 of lithium chloride in the rat, Acta Pharmacol. Toxicol. 47 (5) (1980) 351–354.
[68] O.I. Abdel Hamid, E.M. Ibrahim, M.H. Hussien, S.A. ElKhateeb, The molecular mechanisms of lithium-induced cardiotoxicity in male rats and its amelioration by N-acetyl cysteine, Hum. Exp. Toxicol. 39 (5) (2020) 696–711, https://doi.org/10.1177/0960327119897759.
[69] S. Strbe, S. Gojkovic, I. Krezic, H. Zizek, H. Vranes, I. Barisic, et al., Over-dose lithium toxicity as an occlusive-like syndrome in rats and gastric pentadecapeptide BPC 157, Biomedicines 9 (11) (2021) 1506, https://doi.org/10.3390/biomedicines9111506.
[70] C.E. Rudd, GSK-3 inhibition as a therapeutic approach against SARs CoV2: dual benefit of inhibiting viral replication while potentiating the immune response, Front. Immunol. 11 (1638) (2020), https://doi.org/10.3389/fimmu.2020.01638.
[71] N.M. Pai, V. Malyam, M. Murugesan, S. Ganjekar, S. Moirangthem, G. Desai, Lithium toxicity at therapeutic doses as a fallout of COVID-19 infection: a case series and possible mechanisms, Int. Clin. Psychopharmacol. 37 (1) (2022) 25–28, https://doi.org/10.1097/YIC.0000000000000379.
[72] K. Suwanwongse, N. Shabarek, Lithium toxicity in two coronavirus disease 2019 (COVID-19) patients, Cureus 12 (5) (2020), https://doi.org/10.7759/cureus.8384.
[73] M. Ott, B. Stegmayr, E. Salander Renberg, U. Werneke, Lithium intoxication: incidence, clinical course and renal function–a population-based retrospective cohort study, J. Psychopharmacol. 30 (10) (2016) 1008–1019, https://doi.org/10.1177/0269881116652577.
[74] G.C. Manzoni, G. Bono, M. Lanfranchi, G. Micieli, M.G. Terzano, G. Nappi, Lithium carbonate in cluster headache: assessment of its short- and long-term therapeutic efficacy, Cephalalgia 3 (2) (1983) 109–114.